Eurasian Chem.-Technol. J. 27 (2026) 93–103
The journal of the Institute of Combustion Problems https://ect-journal.kz

https://doi.org/10.18321/ectj1686

Molecular Docking Analysis of Flavonoids from *Verbascum* Species Against Key Antidiabetic Targets: α-Glucosidase and Dipeptidyl Peptidase-IV (DPP-IV)

Asya Tawfiq[1], Aydin Karabulut[2], Balakyz Yeskaliyeva[3], Ahmet Beyatli[4]*

[1]Tikrit University, College of Education for Women, Department of Chemistry, Tikrit, Iraq
[2]Department of Immunology, Hamidiye Health Science Institute, University of Health Sciences, Istanbul, Türkiye
[3]Faculty of Chemistry and Chemical Technology, Al-Farabi Kazakh National University, Almaty, 050040, Kazakhstan
[4]University of Health Sciences, Department of Medicinal and Aromatic Plants, 34668 Üsküdar, Istanbul, Türkiye

Article info

Received:
10 September 2025

Received in revised form:
2 November 2025

Accepted:
14 February 2026

Keywords:
Molecular docking
Diabetes
Flavonoids
Verbascum
Enzymes

Abstract

Diabetes is one of the most significant global health challenges. With synthetic drugs causing side effects, researchers are turning to natural alternatives for prevention and treatment. This study used molecular docking to predict the interaction of flavonoids from *Verbascum* spp. and their affinity for binding to α-glucosidase (3WY1) and DPP-IV (5J3J) enzymes. Binding energies, hydrogen bond interactions, and hydrophobic contacts at the active sites were analyzed. Kaempferide stood out against α-glucosidase with the lowest binding energy (–5.03 kcal/mol), forming strong hydrogen bonds to GLU231 (1.70 Å), LEU300 (1.95 Å), and ASN301 (2.00 Å). Luteolin 7-*O*-β-D-glucopyranoside showed weaker binding (–3.37 kcal/mol) with bonds to GLU383 (1.88, 2.29 Å) and TRP394 (2.45 Å). For DPP-IV, luteolin had the best affinity (–6.01 kcal/mol), creating five hydrogen bonds with GLY335 (1.92, 2.11 Å), SER277 (2.08 Å), TRP337 (2.82 Å), and SER275 (2.99 Å). These results position kaempferide and luteolin as promising candidates for developing natural antidiabetic agents from *Verbascum* species.

1. Introduction

Diabetes mellitus is a prevalent and complex metabolic disorder characterized by persistent hyperglycemia due to impaired insulin secretion, insulin action, or a combination of both [1, 2]. Its global incidence continues to escalate, with recent estimates indicating that approximately 589 million adults are affected worldwide [3]. The condition is associated with serious complications, including cardiovascular disease, neuropathy, nephropathy, and retinopathy, which significantly contribute to morbidity and mortality [4]. Management strategies primarily aim to control blood glucose levels, especially postprandial glucose spikes, which are critical in reducing long-term diabetic complications [5].

Among various therapeutic approaches, inhibition of key enzymes involved in carbohydrate digestion and incretin hormone regulation (namely α-glucosidase and dipeptidyl peptidase-IV (DPP-IV)) has proven effective in lowering post-meal blood glucose levels. α-Glucosidase inhibitors delay carbohydrate breakdown in the gut, decreasing glucose absorption, while DPP-IV inhibitors prolong the activity of incretins, thus enhancing insulin secretion. Despite their clinical benefits, current synthetic inhibitors often induce adverse effects such as gastrointestinal discomfort, highlighting the need for discovering safer, plant-based alternatives [6, 7].

Verbascum L. is a genus belonging to the family Scrophulariaceae, consisting of approximately 360 species distributed primarily throughout temperate regions of the Northern Hemisphere. The genus has its greatest species diversity centered in Türkiye and Iran, part of the Irano-Turanian phytogeographic region, but is also widespread across Europe, North

*Corresponding author.
E-mail address: ahmet.beyatli@sbu.edu.tr

Africa, and parts of Asia. *Verbascum* species are typically herbaceous plants characterized by rosulate, biennial, or perennial growth forms, with yellow flowers arranged in thyrse or raceme inflorescences. The genus exhibits a high rate of endemism, particularly in Türkiye, which houses around 235 species, many of which are endemic. *Verbascum* species have also been naturalized in other parts of the world, including North America, where some species such as *V. thapsus* are common. The diverse habitats and wide geographical distribution emphasize the genus's adaptability and ecological importance [8–10].

Recent studies highlight that flavonoids from various medicinal plants exhibit strong antidiabetic effects in both *in vitro* and *in vivo* models by regulating glucose levels [11–13]. *Verbascum* spp., has been historically employed in traditional medicine systems worldwide. Its widespread use spans treatment of respiratory ailments, wounds, inflammatory conditions, and metabolic disorders, including diabetes [14]. Notably, *Verbascum* species are rich in bioactive phytochemicals, particularly flavonoids, and iridoids, which have been associated with antimicrobial, antioxidative, anti-inflammatory, and antidiabetic effects [15–20].

This study employs molecular docking to investigate how flavonoids from *Verbascum* bind to α-glucosidase and DPP-IV enzymes. The simulations reveal the compounds' inhibitory potential through binding affinities, hydrogen bonds, and hydrophobic contacts at the active sites. Previous work shows flavonoids like luteolin and apigenin with strong docking scores against these targets, backing their promise as natural antidiabetic options [11]. Overall, the research links traditional ethnobotanical insights with computational methods to pinpoint effective inhibitors from *Verbascum* species. The results lay groundwork for developing plant-derived therapies as safer, more effective alternatives to synthetic diabetes drugs.

2. Methodology

2.1. Protein preparation

The crystal structures of human intestinal α-glucosidase (PDB ID: 3WY1) and human Dipeptidyl Peptidase-IV (PDB ID: 5J3J) enzymes were downloaded from the RCSB Protein Data Bank. Both protein structures were preprocessed using UCSF ChimeraX (v1.7) software prior to preparation for molecular docking studies. During this process, all non-standard residues, such as cofactors, crystallization fluids, anions/cations, and water molecules, were removed from the structure. The 5J3J structure consists of two chains, A and B; in our study, only chain A, which contains the catalytic domain, was used, and chain B was removed from the structure. Subsequently, polar hydrogen bonds were added to the protein structures, and Kollman charges were assigned. The final prepared protein structures were converted to PDBQT format using the AutoDock 4.2 toolkit (MGLTools) (Fig. 1).

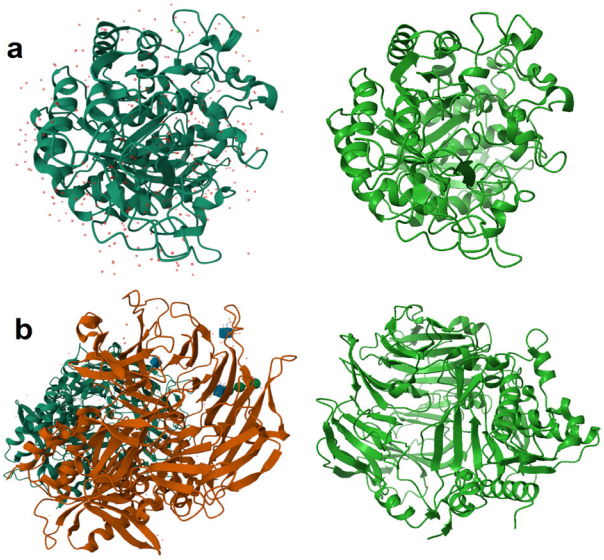

Fig. 1. Crystal structures of the target proteins used in the study: (a) – α-Glucosidase (3WY1); (b) – DPP-IV (5J3J).

2.2. Ligand preparation

The three-dimensional structures of flavonoid compounds (e.g., kaempferide, luteolin 7-*O*-β-D-glucopyranoside, quercetin 3-*O*-β-D-glucopyranoside, quercetin, luteolin) belonging to the *Verbascum* species evaluated in the study were downloaded from the NCBI PubChem database. The compound structures, initially in SDF (Structure-Data File) format, were subjected to energy minimization (MMFF94 force field) using Avogadro (v1.2.0) software and converted to Mol2 format. Rotatable bonds were defined using MGLTools. Finally, PDBQT input files were created for each ligand (Fig. 2).

2.3. Molecular docking

AutoDock 4.2 software was used to predict ligand-protein interactions. For the docking process, a grid box was defined to cover the catalytic region of each protein. For α-Glucosidase (3WY1), the grid box center was placed at coordinates x = –12.492,

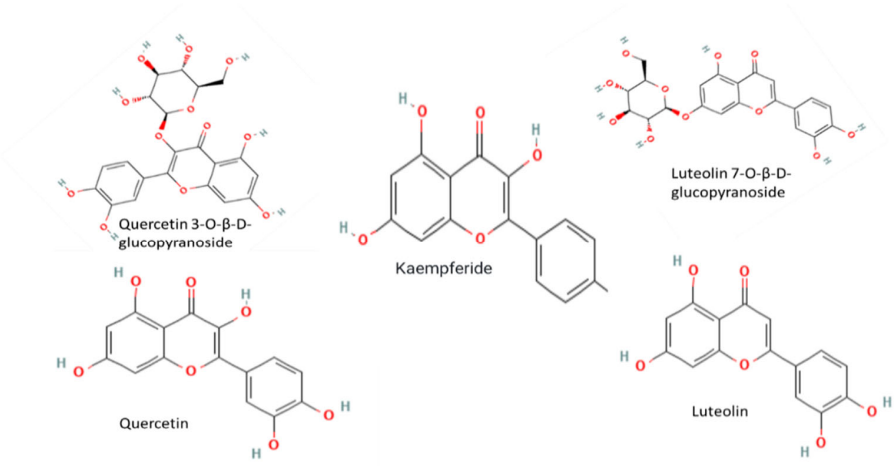

Fig. 2. 2D Chemical structures of the flavonoid compounds from *Verbascum* spp. retrieved from Pubchem database.

y = –35.602, z = –18.229. The grid center and dimensions were specifically chosen to encompass the deep catalytic pocket of 3WY1, ensuring the inclusion of critical catalytic residues such as Asp518, Asp616, and His674. This site was further validated by the location of the co-crystallized ligand in the PDB structure, which served as the reference for determining the optimal docking space. The box dimensions were set to 60x60x60 grid points, and the grid spacing was set to 0.375 Å. For DPP-IV (5J3J), the grid box center was positioned at coordinates x = –10.962, y = –6.936, z = –12.753, based on the residues in the catalytic triad (Ser630, Asp708, His740). The box dimensions were set to 60x60x60 grid points and the grid spacing to 0.375 Å. To validate the docking protocol, the co-crystallized ligands were re-docked into the active sites of α-glucosidase (3WY1) and DPP-IV (5J3J). The Root Mean Square Deviation (RMSD) values were calculated to be 1.24 Å and 1.42 Å, respectively. These values, well below the 2.0 Å threshold, confirm the reliability and accuracy of the docking parameters used in this study.

After defining the grid parameters, the AutoGrid 4 program was run to generate mapping files for each protein. The binding conformations of the ligands to the proteins were calculated using the Lamarckian Genetic Algorithm (LGA). One hundred different runs were performed for each ligand-protein pair, and other parameters were left at their default values. The docking outputs were evaluated based on parameters such as binding energy (kcal/mol) and inhibition constant (Ki). In this study, hydrogen bond interactions were defined based on a distance threshold of up to 3.5 Å, which accounts for both strong (below 3.0 Å) and moderate-to-weak interactions that contribute to the overall stability of the ligand-protein complex [21].

2.4. Visualization and analysis of docking results

Conformations with the lowest binding energy were analyzed and visualized using ChimeraX and Discovery Studio Visualizer (v2021) software. These tools were used to examine ligand-protein interactions (hydrogen bonds, hydrophobic interactions, π-π stacking, etc.) in detail and to generate figures of publishable quality.

3. Results and Discussion

3.1. Molecular docking analysis of 3WY1 enzyme with Verbascum spp. compounds

In molecular docking studies, binding energy is used as a fundamental parameter to evaluate the stability and affinity of protein-ligand interactions. In our study, the binding energies obtained from the molecular docking analysis of compounds derived from *Verbascum* species with α-glucosidase (3WY1) are presented in Table 1. Negative binding energy indicates that the ligand-protein complex is stable [22]. The fact that all compounds have negative binding energy shows that they form stable complexes with 3WY1.

Table 1. The binding energy of 3WY1 enzyme with plant compounds.

Compounds	Binding energy kcal/mol
Kaempferide	–5.03
Luteolin 7-*O*-β-D-glucopyranoside	–3.37
Quercetin 3-*O*-β-D-glucopyranoside	–3.69
Quercetin	–4.81
Luteolin	–4.95

When examining the binding energies, kaempferide (–5.03 kcal/mol) exhibited the lowest and therefore the most favorable value. This result suggests that kaempferide has the strongest interaction with the enzyme and may represent a promising inhibitor candidate. It was followed by luteolin (–4.95 kcal/mol), quercetin (–4.81 kcal/mol), quercetin 3-*O*-β-D-glucopyranoside (–3.69 kcal/mol), and luteolin 7-*O*-β-D-glucopyranoside (–3.37 kcal/mol) [20, 21]. The relatively higher (less negative) binding energy of luteolin 7-*O*-β-D-glucopyranoside indicates that this compound has a lower binding affinity for the enzyme compared with the other compounds.

To further support these results, the molecular interactions established between the compounds and the 3WY1 active site were visualized and analyzed using Discovery Studio and ChimeraX software (Table 2). Kaempferide formed hydrogen bonds with the amino acid residues GLU231, LEU300, and ASN301, with bond lengths of 1.70, 1.95, and 2.00 Å, respectively (Fig. 3a). Visualization using ChimeraX also revealed hydrogen bond interactions with LYS225, GLU231, and LEU300 (Fig. 3b). Luteolin 7-*O*-β-D-glucopyranoside formed hydrogen bonds with residues GLU383 and TRP394 (Fig. 4). Quercetin 3-*O*-β-D-glucopyranoside formed six different hydrogen bonds with multiple residues such as GLY374, ARG429, ALA343, and GLU432, exhibiting a remarkable interaction network (Fig. 5). Quercetin interacts with five hydrogen bonds and is located in regions of catalytic importance, such as GLY399, GLU377, and ARG429 (Fig. 6). Luteolin formed four hydrogen bonds with LEU277, GLU396, and GLY399 (Fig. 7).

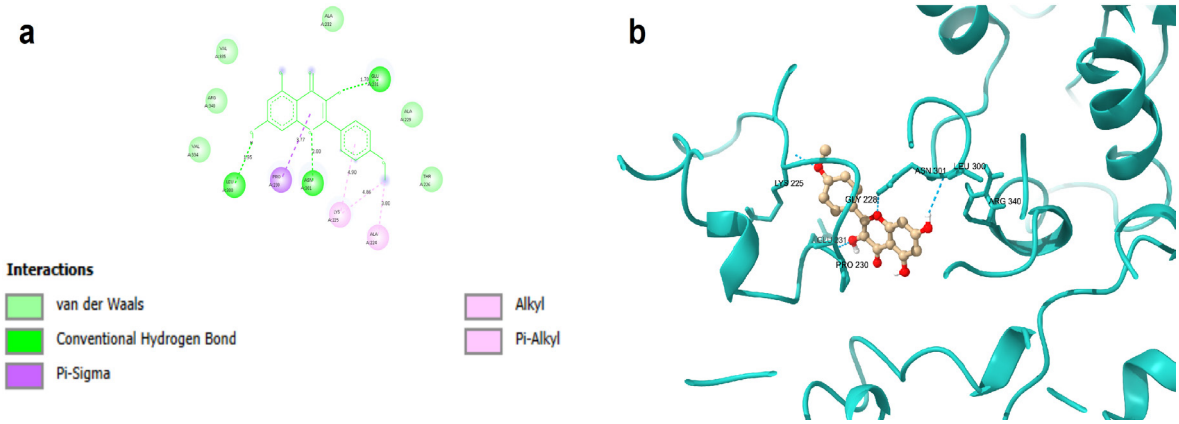

Fig. 3. Molecular interaction between the kaempferide and the active site of the α-glucosidase (3WY1) enzyme. (a) Two-dimensional interaction diagram: Green dashed lines indicate critical hydrogen bonds between kaempferide and the enzyme; pink circles indicate hydrophobic interactions. (b) Three-dimensional structural model: Shows how kaempferide (stick model) binds to the enzyme's active site (ribbon diagram).

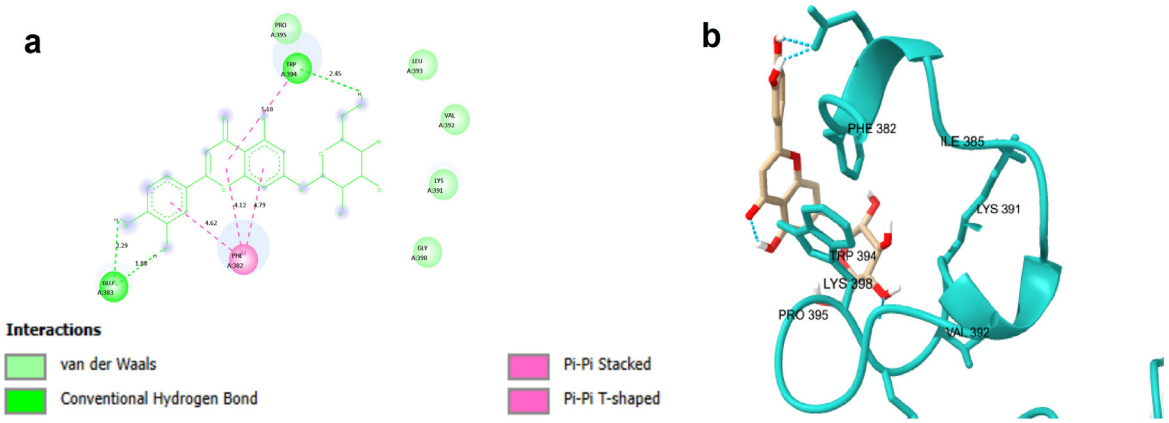

Fig. 4. Interaction of the luteolin 7-*O*-β-D-glucopyranoside with the active site of α-glucosidase (3WY1). (a) Two-dimensional interaction diagram showing hydrogen bonds (green dashed lines) and hydrophobic interactions (pink circles). (b) Three-dimensional structural model showing the binding position of the compound (stick model) to the enzyme's active site (ribbon model).

Table 2. Hydrogen bond formation and interacting residues of enzyme 3WY1 with the prepared compound that were analyzed by AutoDock 4.2 and Discover studio.

Compounds	Interacting residues	H-bond	Distance (A) H-bond
Kaempferide	$GLU_{A:231}$, $LEU_{A:300}$, and $ASN_{A:301}$ (HB), $PRO_{A:230}$ (Pi-Sigma), $ALA_{A:224}$ and $LYS_{A:225}$ (Alkyl), $LYS_{A:225}$ (Pi-Alkyl)	3	1.70, 1.95, 2.00
Luteolin 7-O-β-D-glucopyranoside	$GLU_{A:383}$, $GLU_{A:383}$ and $TRP_{A:394}$ (HB), PHE_{A382} (Pi-Pi Stacked), $TRP_{A:394}$ (Pi-Pi T-shaped)	3	1.88, 2.29, 2.45
Quercetin 3-O-β-D-glucopyranoside	$GLY_{A:374}$, $GLY_{A:374}$, $ARG_{A:429}$, $ALA_{A:343}$, $GLU_{A:432}$ and $GLU_{A:432}$ (HB), $PRO_{A:347}$ (Pi-Alkyl)	6	1.77, 2.46, 2.07, 2.12, 1.87,2.07
Quercetin	$GLY_{A:399}$, $GLY_{A:399}$, $GLY_{A:402}$, $GLU_{A:377}$, $ARG_{A:429}$ (HB), $LYS_{A:398}$ (Pi-Alkyl), $ASP_{A:379}$ (pi-Anion)	5	1.81, 1.96, 2.06, 2.26, 2.86
Luteolin	$LEU_{A:227}$, $LEU_{A:227}$, $GLU_{A:396}$ and $GLY_{A:399}$(HB), $PHE_{A:397}$ and $PHE_{A:397}$ (Pi-Pi T-shaped), $VAL_{A:335}$, $LYS_{A:398}$, $PRO_{A:230}$ and, $VAL_{A:334}$ (Pi-Alkyl)	3	1.88, 1.98, 2.28, 2.09

(HB) = Hydrogen Bond interaction.

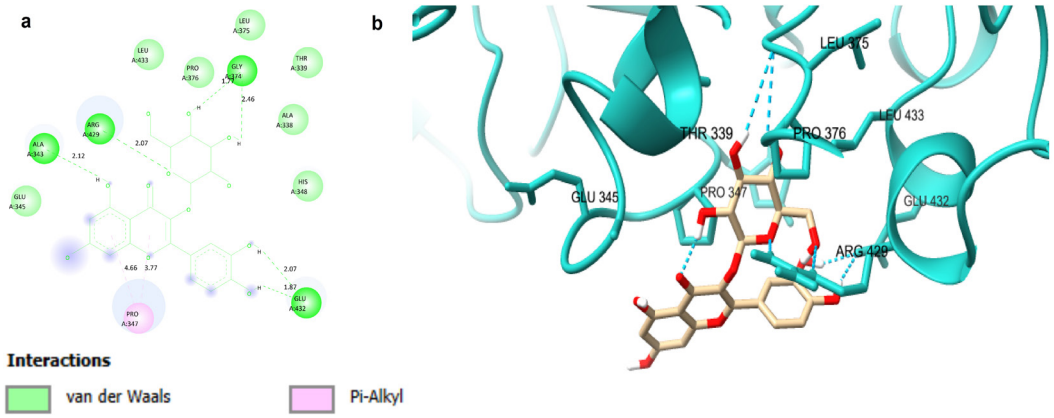

Fig. 5. Interaction of the Quercetin 3-*O*-β-D-glucopyranoside with the active site of α-glucosidase (3WY1). (a) Two-dimensional interaction diagram showing hydrogen bonds (green dashed lines) and hydrophobic interactions (pink circles). (b) Three-dimensional structural model showing the binding position of the compound (stick model) to the enzyme's active site (ribbon model).

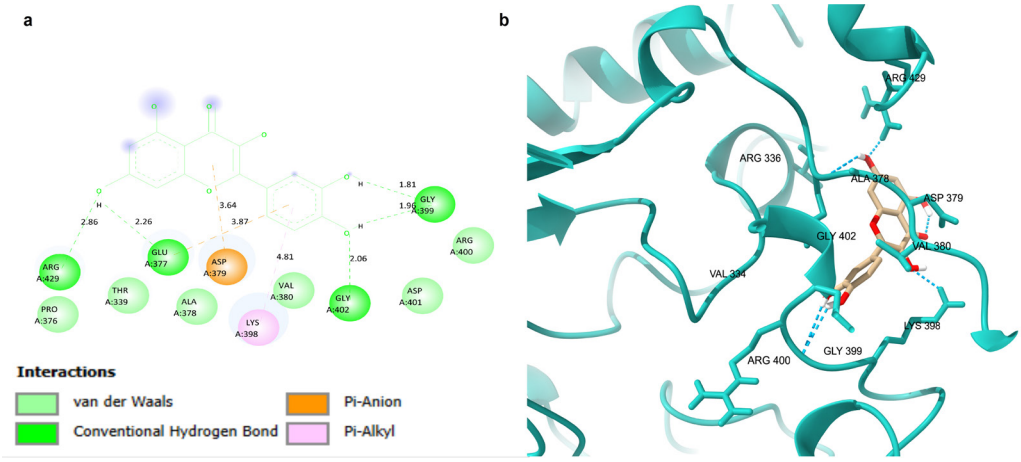

Fig. 6. Interaction of the Quercetin with the active site of α-glucosidase (3WY1). (a) Two-dimensional interaction diagram showing hydrogen bonds (green dashed lines) and hydrophobic interactions (pink circles). (b) Three-dimensional structural model showing the binding position of the compound (stick model) to the enzyme's active site (ribbon model).

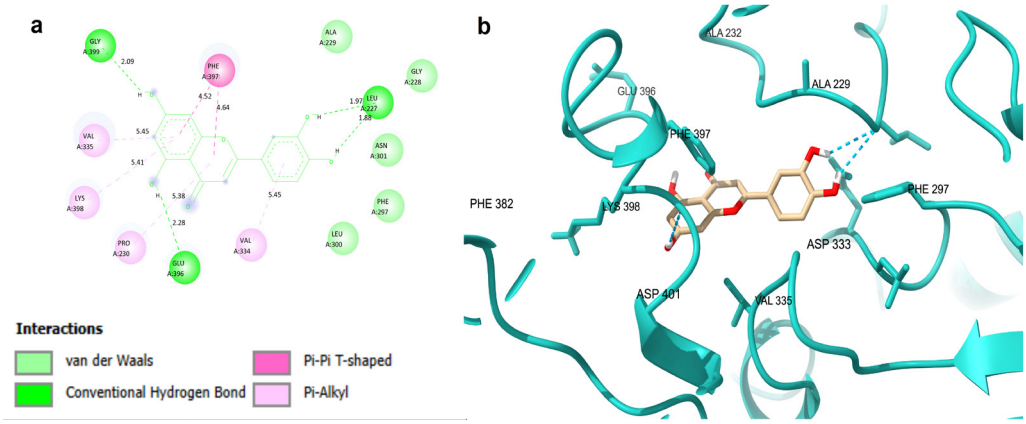

Fig. 7. Interaction of the Luteolin with the active site of α-glucosidase (3WY1). (a) Two-dimensional interaction diagram showing hydrogen bonds (green dashed lines) and hydrophobic interactions (pink circles). (b) Three-dimensional structural model showing the binding position of the compound (stick model) to the enzyme's active site (ribbon model).

The hydrogen bond lengths were found to be within the range of 1.5–2.6 Å, which is considered ideal in the literature [21]. In particular, the short and strong 1.70 Å hydrogen bond formed by kaempferidin with GLU231 is considered to contribute significantly to the high stability and low binding energy of this complex. Considering that bonds longer than 3.0 Å are generally considered weak interactions [23], it was concluded that all studied compounds formed meaningful and strong bonds with the 3WY1 enzyme. In light of all these findings, it was concluded that kaempferide is a promising natural compound as an α-glucosidase inhibitor.

3.2. Hydrophobic interaction

Hydrophobic interactions play a critical role in the stabilization of ligand-protein complexes, as do hydrogen bonds [24]. It has been determined that the binding between our compounds and the 3WY1 (α-glucosidase) enzyme is also supported by such interactions. Analysis revealed a total of four hydrophobic interactions between kaempferide and the 3WY1 enzyme: PRO230 (Pi-Sigma), ALA224 (Alkyl), and LYS225 (Alkyl and Pi-Alkyl) (Fig. 3a). In particular, the participation of the PRO230 and LYS225 residues in hydrogen bonds has created a very strong and versatile binding network for this compound, significantly increasing the stability of the complex.

In contrast, fewer hydrophobic interactions were observed between luteolin 7-*O*-β-D-glucopyranoside and the enzyme. This compound has established hydrophobic interaction only with the PHE382 (Pi-Pi Stacking) and TRP394 (Pi-Pi T-Shaped) residues (Fig. 4a). The number and variety of hydrophobic interactions are consistent with the previously mentioned binding energy results. Kaempferide's lower (more negative) binding energy and its more extensive interaction network with the enzyme's active site via both hydrogen and hydrophobic interactions make it a more stable and potent binder compared to Luteolin 7-*O*-β-D-glucopyranoside. The molecule's relatively larger structure may also have facilitated this extensive interaction. All these findings further support kaempferide as a promising α-glucosidase inhibitor candidate for the treatment of Type 2 Diabetes Mellitus.

3.3. Molecular docking analysis of 5J3J enzyme with Verbascum spp. compounds

Molecular interactions between compounds obtained from *Verbascum* spp. and the DPP-IV enzyme (5J3J) were analyzed using the AutoDock 4.2 program, and binding energies, a key indicator of complex stability, were calculated. Upon examining the calculated binding energies, luteolin was found to have the lowest (most favorable) binding energy with a value of –6.01 kcal/mol (Table 3).

Table 3. The binding energy of 5J3J enzyme with extract compounds.

Compounds	Binding energy kcal/mol
Kaempferide	–5.75
Luteolin 7-*O*-β-D-glucopyranoside	–3.05
Quercetin 3-*O*-β-D-glucopyranoside	–4.56
Quercetin	–5.84
Luteolin	–6.01

Consistent with the literature, a lower binding energy indicates that the protein-ligand complex binds with higher affinity and therefore stronger interaction [25]. This suggests that luteolin is the most promising binding compound and a potential inhibitor candidate for the 5J3J enzyme. Luteolin formed a hydrogen bond with SER275 at a distance of 2.99 Å, representing a stabilizing interaction within the binding pocket. In contrast, Luteolin 7-*O*-β-D-glucopyranoside exhibited a higher (less negative) binding energy of –3.05 kcal/mol, indicating weaker affinity toward the enzyme.

To contextualize these results, our findings were compared with published docking data for standard inhibitors. For α-glucosidase (3WY1), the reference inhibitor acarbose has been reported to exhibit binding energies ranging from –4.5 to –5.8 kcal/mol in similar docking studies [20, 21]. Our lead compound, kaempferide (–5.03 kcal/mol), showed a comparable affinity. For DPP-IV (5J3J), standard inhibitors like sitagliptin generally show higher binding affinities (approximately –8.0 kcal/mol) [11]. This suggests that while the investigated flavonoids demonstrate promising inhibitory potential, particularly against α-glucosidase, they serve as moderate inhibitors for DPP-IV compared to synthetic drugs.

3.4. Hydrogen bond interactions

A detailed analysis of hydrogen bond interactions between the compounds and the 5J3J (DPP-IV) enzyme is summarized in Table 4. Visualization of these interactions revealed minor differences between the results of different software algorithms (Discovery Studio and ChimeraX).

Kaempferide formed hydrogen bonds with GLU91, GLY99, and LYS71 according to Discovery Studio, and with GLY99 and ILE102 according to ChimeraX (Fig. 8). Luteolin 7-*O*-β-D-glucopyranoside was the compound that formed the highest number of hydrogen bonds; the Discovery Studio analysis detected six hydrogen bonds with ILE513, ASP515, GLN612, and LYS615, while ChimeraX detected five (Fig. 9). Quercetin 3-*O*-β-D-glucopyranoside interacts with multiple residues such as VAL459, GLU408, LEU410, LYS463, and TRP62, forming eight (Discovery Studio) and four (ChimeraX) hydrogen bonds (Fig. 10). Quercetin formed four hydrogen bonds with VAL270, SER277, TRP337, and TYR330, and both software programs showed consistent results (Fig. 11). Luteolin formed five hydrogen bonds each with the residues GLY335, SER277, TRP337, and SER275, and again, consistency was observed between the two software programs (Fig. 12).

When evaluating hydrogen bond lengths, the short 1.62 Å bond formed by luteolin 7-*O*-β-D-glucopyranoside with ILE513 indicates a strong interaction. In contrast, the 2.99 Å bond observed for luteolin approaches the weak interaction threshold of 3.0 Å reported in the literature [23]. Overall, the hydrogen bond lengths of all compounds fall within the ideal range of 1.5–2.6 Å [21], contributing to the stability of the complexes.

Table 4. Hydrogen bond formation and interacting residues of enzyme 5J3J with the prepared compound that were analyzed by AutoDock 4.2 and Discover studio.

Compounds	Interacting residues	H-bond	Distance(A) H-bond
Kaempferide	$GLU_{A:91}$, $GLY_{A:99}$ and $LYS_{A:71}$ (HB), $ILE_{A:102}$ (Pi-Sigma), $PHE_{A:95}$ (Pi-LonePair, $ILE_{A:102}$ (PiAlkyl)	3	2.02, 2.18, 2.26
Luteolin 7-*O*-β-D-glucopyranoside	$ILE_{A:513}$, $ASP_{A:515}$, $ASP_{A:515}$, $GLN_{A:612}$, $LYS_{A:615}$ and $LYS_{A:615}$ (HB), $PHE_{A:516}$(Pi-Pi T-shaped), $ILE_{A:517}$(Pi-Alkyl)	5	1.62, 2.05, 2.12, 2.29, 2.02, 2.25
Quercetin 3-*O*-β-D-glucopyranoside	$VAL_{A:459}$, $GLU_{A:408}$, $LEU_{A:410}$, $LEU_{A:408}$, $LYS_{A:463}$, $LYS_{A:463}$, $LYS_{A:463}$ and $TRP_{A:62}$ (HB), $PHE_{A:461}$ and $TRP_{A:62}$ (Carbon HB)	8	2.01, 2.84, 2.16, 2.32, 1.87, 2.10, 2.62, 2.25
Quercetin	$VAL_{A:270}$, $SER_{A:277}$, $TRP_{A:337}$ and $TYR_{A:330}$ (HB), $THR_{A:283}$ (Pi-Donar HB), $PHE_{A:222}$(Pi-Pi T-shaped), $ALA_{A:282}$ (Pi-Alkyl), $ILE_{A:285}$ (Unfavorable Donor-Donor	4	1.97, 2.19, 2.51, 2.95
Luteolin	$GLY_{A:335}$, $GLY_{A:335}$, $SER_{A:277}$, $TRP_{A:337}$ and $SER_{A:275}$ (HB), $THR_{A:283}$ (Pi-Donar (HB), $ILE_{A:285}$ and $ALA_{A:282}$ (Pi-Alkyl)	5	1.92, 2.11, 2.08, 2.82, 2.99

(HB) = Hydrogen Bond interaction.

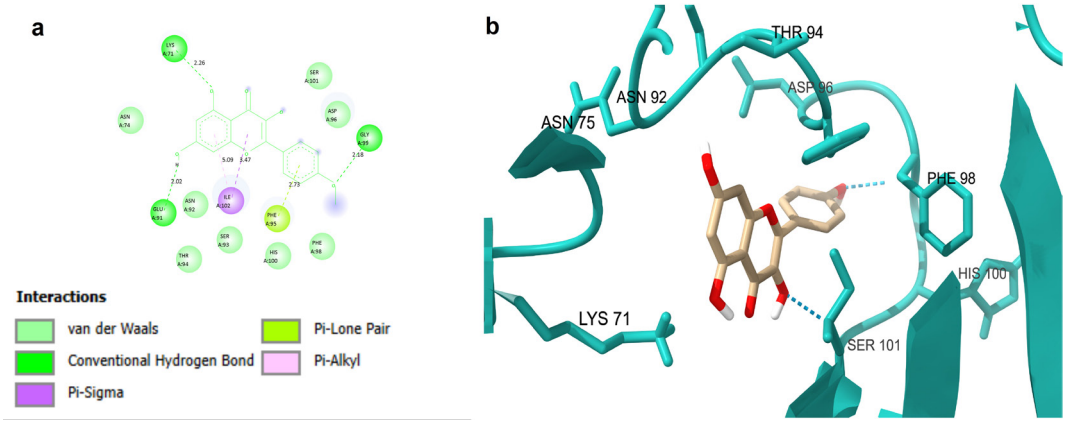

Fig. 8. Interaction of Kaempferide with the active site of DPP-IV (5J3J). (a) Two-dimensional interaction diagram showing hydrogen bonds (green dashed lines) and hydrophobic interactions (pink circles). (b) Three-dimensional structural model showing the binding position of the compound (stick model) to the enzyme's active site (ribbon model).

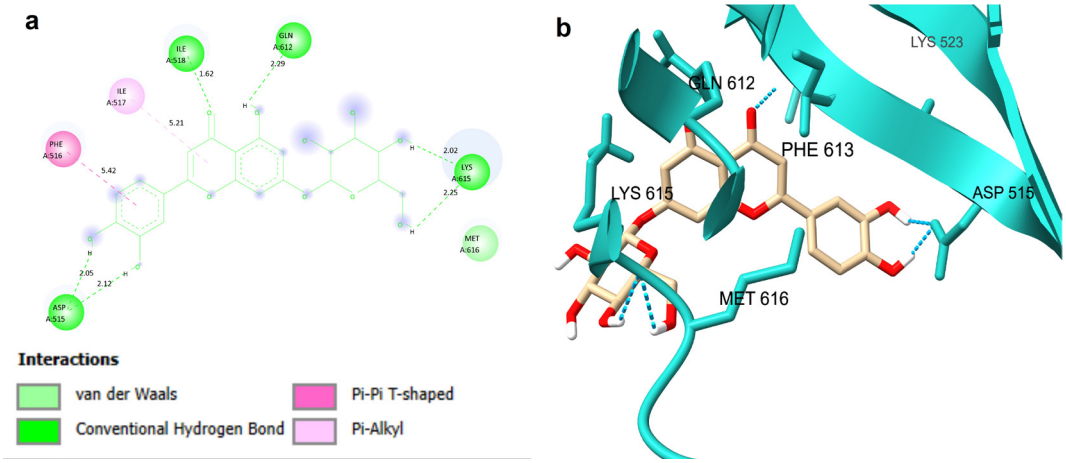

Fig. 9. Interaction of Luteolin 7-*O*-β-D-glucopyranoside with the active site of DPP-IV (5J3J). (a) Two-dimensional interaction diagram showing hydrogen bonds (green dashed lines) and hydrophobic interactions (pink circles). (b) Three-dimensional structural model showing the binding position of the compound (stick model) to the enzyme's active site (ribbon model).

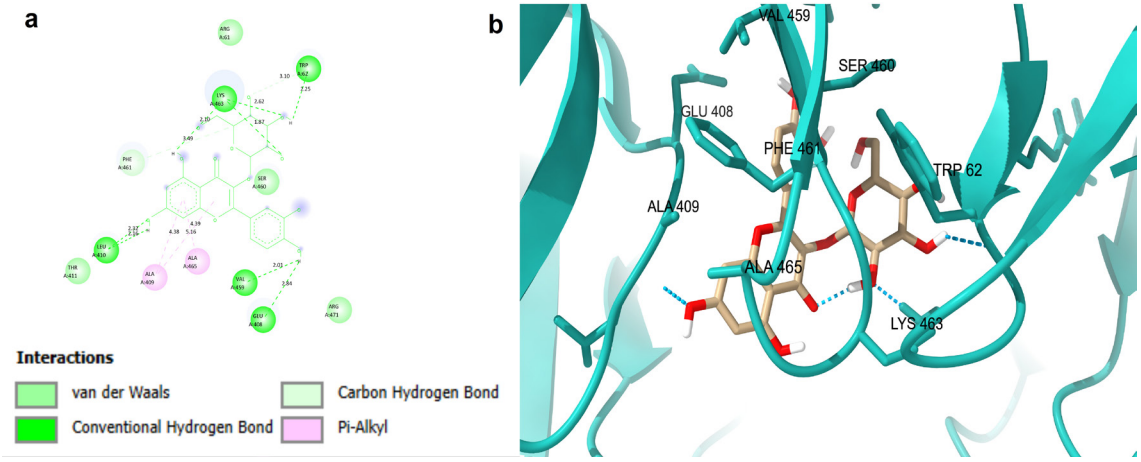

Fig. 10. Interaction of Quercetin 3-*O*-β-D-glucopyranoside with the active site of DPP-IV (5J3J). (a) Two-dimensional interaction diagram showing hydrogen bonds (green dashed lines) and hydrophobic interactions (pink circles). (b) Three-dimensional structural model showing the binding position of the compound (stick model) to the enzyme's active site (ribbon model).

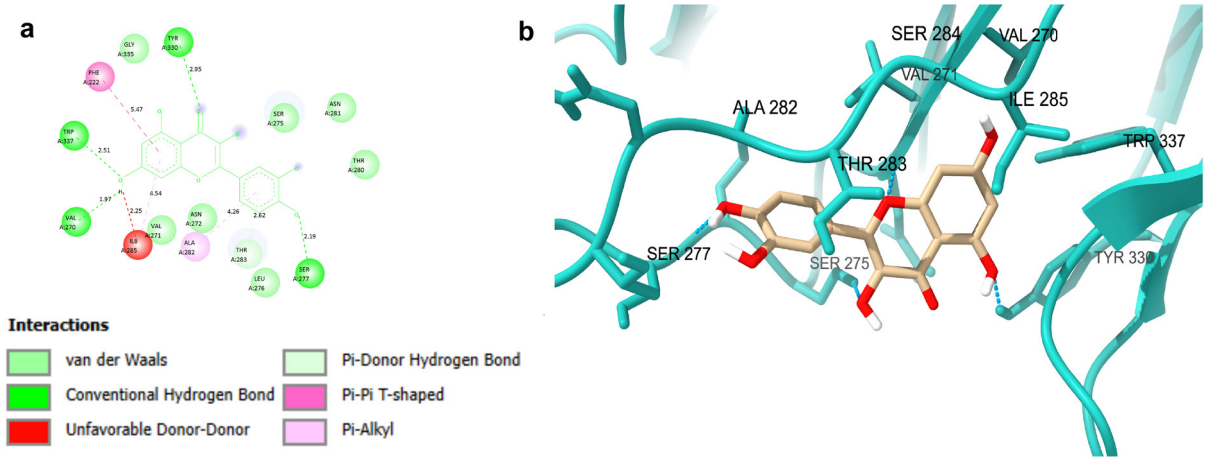

Fig. 11. Interaction of Quercetin with the active site of DPP-IV (5J3J). (a) Two-dimensional interaction diagram showing hydrogen bonds (green dashed lines) and hydrophobic interactions (pink circles). (b) Three-dimensional structural model showing the binding position of the compound (stick model) to the enzyme's active site (ribbon model).

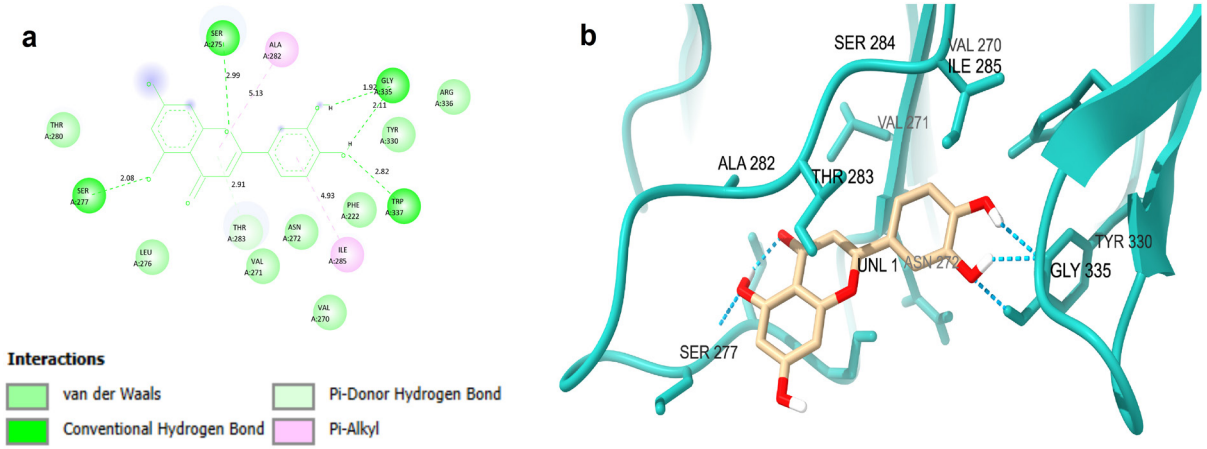

Fig. 12. Interaction of Luteolin with the active site of DPP-IV (5J3J). (a) Two-dimensional interaction diagram showing hydrogen bonds (green dashed lines) and hydrophobic interactions (pink circles). (b) Three-dimensional structural model showing the binding position of the compound (stick model) to the enzyme's active site (ribbon model).

3.5. Hydrophobic interactions

It has been determined that hydrophobic interactions also play an important role in the stabilization of molecular interactions between compounds and the 5J3J (DPP-IV) enzyme. Kaempferide established three different hydrophobic interactions (Pi-Sigma, Alkyl, and Pi-Alkyl) with the enzyme's ILE102 and PHE95 residues (Fig. 8a). The fact that the ILE102 residue also forms a hydrogen bond created a versatile and robust binding network for kaempferide. Luteolin 7-*O*-β-D-glucopyranoside, on the other hand, formed two hydrophobic interactions with ILE517 (Pi-Alkyl) and PHE516 (Pi-Pi T-shaped) (Fig. 9a). Luteolin exhibits three hydrophobic interactions with THR283 (Pi-Donor Hydrogen Bond), ILE282, and ILE285 (Alkyl) (Fig. 12a).

When these findings are evaluated together with the binding energy results, it is thought that the hydrophobic interactions in luteolin, which has the lowest binding energy, contribute significantly to the overall stability of the complex. The fewer hydrophobic interactions established with Luteolin 7-*O*-β-D-glucopyranoside are consistent with the relatively higher binding energy of this compound. In conclusion, considering both the strong binding energy and the multifaceted hydrophobic interactions, luteolin is considered the most promising inhibitor candidate for the 5J3J enzyme. Future studies should benchmark these binding affinities against established inhibitors like acarbose (α-glucosidase) or sitagliptin (DPP-IV) through in vitro assays to assess relative efficacy.

4. Conclusion

The molecular docking results demonstrated that flavonoids from *Verbascum* spp. effectively bind to both α-glucosidase and DPP-IV enzymes. All investigated compounds formed stable complexes characterized by negative binding energies, hydrogen bonding, and hydrophobic interactions. Kaempferide exhibited the strongest affinity toward α-glucosidase (–5.03 kcal/mol), driven by strong interactions within the active site, whereas luteolin showed the highest binding affinity toward DPP-IV (–6.01 kcal/mol). Other flavonoids, such as quercetin (–4.81 and –5.5 kcal/mol), as well as glycosylated derivatives, also demonstrated notable but comparatively weaker interactions, highlighting the overall antidiabetic potential of this group of compounds. These *in silico* findings suggest that kaempferide and luteolin may represent promising candidates for type 2 diabetes management, with additional contributions from other flavonoids. Further studies, including *in vitro* enzyme inhibition assays, molecular dynamics simulations, and detailed mechanistic investigations, are required to validate and further elucidate these results.

References

[1]. American Diabetes Association Professional Practice Committee; 2. Diagnosis and Classification of Diabetes: Standards of Care in Diabetes—2025. Diabetes Care 1 January 2025; 48 (Supplement_1): S27–S49. DOI: 10.2337/dc25-S002

[2]. World Health Organization, Diabetes – WHO Fact Sheet, World Health Organization (2025). Available at: https://www.who.int/news-room/fact-sheets/detail/diabetes (Accessed: 30.09.2025).

[3]. International Diabetes Federation, The Diabetes Atlas, (2025). Available at: https://diabetesatlas.org/ (Accessed: 30.09.2025).

[4]. O.I. Aruoma, V.S. Neergheen, T. Bahorun, L-S. Jen, Free radicals, antioxidants and diabetes: Embryopathy, retinopathy, neuropathy, nephropathy and cardiovascular complications, *Neuroembryology Aging* 4 (2007) 117–137. DOI: 10.1159/000109344

[5]. A. Ceriello, Postprandial hyperglycemia and diabetes complications: is it time to treat? *Diabetes* 54 (2005) 1–7. DOI: 10.2337/diabetes.54.1.1

[6]. K. Nakamura, H. Oe, H. Kihara, et al., DPP-4 inhibitor and alpha-glucosidase inhibitor equally improve endothelial function in patients with type 2 diabetes: EDGE study, *Cardiovasc. Diabetol.* 13 (2014) 110. DOI: 10.1186/s12933-014-0110-2

[7]. S. Yagi, N. Nilofar, A.I. Uba, et al., Elucidating the chemical profile and biological studies of *Verbascum diversifolium* Hochst. extracts, *Front. Pharmacol.* 15 (2024). DOI: 10.3389/fphar.2024.1333865

[8]. X. Dong, E.M. Mkala, E.S. Mutinda, et al., Taxonomy, comparative genomics of Mullein (*Verbascum*, Scrophulariaceae), with implications for the evolution of *Verbascum* and Lamiales, *BMC Genomics* 23 (2022) 566. DOI: 10.1186/s12864-022-08799-9

[9]. F. Mungan Kılıç, Pollen and seed morphology as taxonomic markers in *Verbascum* taxa based on herbarium specimens of MARIUM, *Diversity* 16 (2024) 443. DOI: 10.3390/d16080443

[10]. WFO, Verbascum L. World Flora Online (2025). Available at: https://www.worldfloraonline.org/taxon/wfo-4000040135 (Accessed: 30.09.2025).

[11]. J.S. Matejić, A.V. Dragićević, M.S. Jovanović, et al., Plant products for musculoskeletal, respiratory, circulatory, and genitourinary disorders in Eastern and South-Eastern Serbia–folk uses comparison with official recommendations, *Rec. Nat. Prod*. 18 (2024) 1–52. DOI: 10.25135/rnp.428.2308.2861

[12]. B. Dereje, A. Nardos, J. Abdela, et al., Antidiabetic activities of 80% methanol extract and solvent fractions of *Verbascum sinaiticum* Benth (Scrophulariaceae) leaves in mice, *J. Exp. Pharmacol.* 15 (2023) 423–436. DOI: 10.2147/JEP.S437991

[13]. W. Khan, M.A. Khan, B. Khan, et al., Evaluation of antidiabetic and antihyperlipidemic effects of methanolic extract of *Verbascum thapsus* in alloxan-induced diabetic albino mice, *Pak. J. Weed Sci. Res.* 29 (2023) 1–8. https://researcherslinks.com/current-issues/Evaluation-of-Antidiabetic-and-Antihyperlipidemic/38/1/6151

[14]. M.M. Nykmukanova, B.K. Eskalieva, G.Sh. Burasheva, et al., Iridoids from *Verbascum marschallianum*, *Chem. Nat. Compd*. 53 (2017) 580–581. DOI: 10.1007/s10600-017-2056-6

[15]. M.M. Nykmukanova, Zh.B. Mukazhanova, K. Kabdysalym, et al., Flavonoids from *Verbascum marschallianum* and *V. orientale*, *Chem. Nat. Compd.* 55 (2019) 937–938. DOI: 10.1007/s10600-019-02852-y

[16]. B. Ozcan, M. Yilmaz, M. Caliskan, Antimicrobial and antioxidant activities of various extracts of *Verbascum antiochium* Boiss. (Scrophulariaceae), *J. Med. Food* 13 (2010). DOI: 10.1089/jmf.2009.0213

[17]. L. Speranza, S. Franceschelli, M. Pesce, et al., Antiinflammatory effects in THP-1 cells treated with verbascoside, *Phytother. Res*. 24 (2010) 1398–1404. DOI: 10.1002/ptr.3173

[18]. J. Pan, Q. Zhang, C. Zhang, et al., Inhibition of dipeptidyl peptidase-4 by flavonoids: Structure–activity relationship, kinetics and interaction mechanism, *Front. Nutr.* 9 (2022) 892426. DOI: 10.3389/fnut.2022.892426

[19]. H. Kondo, K.J. Fujimoto, S. Tanaka, et al., Theoretical prediction and experimental verification on enantioselectivity of haloacid dehalogenase l-DEX YL with chloropropionate, *Chem. Phys. Lett.* 623 (2015) 101–107. DOI: 10.1016/j.cplett.2015.01.053

[20]. A. Bhatia, B. Singh, R. Arora, et al., In vitro evaluation of the α-glucosidase inhibitory potential of methanolic extracts of traditionally used antidiabetic plants, *BMC Complement. Altern. Med*. 19 (2019) 74. DOI: 10.1186/s12906-019-2482-z

[21]. A. Sadiq, U. Rashid, S. Ahmad, et al., Treating hyperglycemia from *Eryngium caeruleum* M. Bieb: In-vitro α-glucosidase, antioxidant, in-vivo antidiabetic and molecular docking-based approaches, *Front. Chem.* 8 (2020) 558641. DOI: 10.3389/fchem.2020.558641

[22]. J.M. Berg, J.L. Tymoczko, G.J. Gatto, L. Stryer, Biochemistry, 9th ed., W.H. Freeman, Macmillan Learning, New York (2019). DOI: 10.1007/978-3-662-54620-8

[23]. P.K. Thallapally, A. Nangia, A Cambridge Structural Database analysis of the C–H Cl interaction: C–H··· Cl− and C–H···Cl–M often behave as hydrogen bonds but C–H···Cl–C is generally a van der Waals interaction, *CrystEngComm* 3 (2001) 114–119. DOI: 10.1039/B102780H

[24]. S.K. Panigrahi, G.R. Desiraju, Strong and weak hydrogen bonds in the protein–ligand interface, *Proteins: Struct., Funct., Bioinf*. 67 (2007) 128–141. DOI: 10.1002/prot.21253

[25]. E.S. Day, S.M. Cote, A. Whitty, Binding efficiency of protein–protein complexes, *Biochemistry* 51 (2012) 9124–9136. DOI: 10.1021/bi301039t